Journal of Engineering Physics and Thermophysics, Vol. 81, No. 1, 2008

EXPERIMENTAL INVESTIGATION OF THE MIXING PERFORMANCE OF A LOBED JET FLOW

Amina Meslem, Ilinca Nastase, and Kamel Abed-Meraim

UDC 532.525.2:517.4

An experimental investigation of flow in a turbulent isothermal air lobed jet is presented. A lobed jet is compared, in the near field, with an isothermal axisymmetric jet with the same exit Reynolds number in terms of dynamics and mixing enhancement. It was found that the streamwise variation of the volumetric flow rate is characterized by a slope is more than twice larger than that for the reference circular jet. This high entrainment rate is governed, at the same time, by the turbulent structures generated by the asymmetric shape of the nozzle and by the high convection in these structures induced by the inner and outer penetration angles of their lobes.

Control of jet flow by passive means has been widely used to improve the combustion efficiency and to reduce the amount of pollutants in mixing chambers. For this purpose, use is made of three-dimensional nozzles, whose shapes were made progressively complex over the last decade to improve the self-induction of the asymmetric coherent structures generated at the nozzle exit.

The use of circular or rectangular tabbed nozzles proved their efficiency in terms of mixing performance compared to rectangular and circular nozzles without tabs [1–4]. Each tab generates a pair of counter-rotating streamwise vortices that modify the turbulent structures of the jet flow, increasing the performance of its mixing with the secondary flow. The geometry of diffuser nozzles has also been oriented towards more complex shapes [5, 6], and it was emphasized in recent works [7, 8] that the lobed nozzle is an extraordinary mixing device.

Through this study, we aim to estimate the mixing performance of a turbulent jet issued from a "daisy" lobed nozzle and to compare it with that for an axisymmetric jet having the same initial volumetric rate and exit area. For this purpose, the dynamic field and the flow characteristics will be analyzed.

Exit Conditions. Turbulent isothermal air jets issued from a circular reference nozzle having diameter D = 40 mm and from a "daisy" lobed nozzle with the same equivalent diameter D_e (Fig. 1) were investigated within an axial distance of $X = 5D_e$. The lobe width and height are λ = 6 mm and H = 15 mm, respectively. The inner and outer penetration angles of the lobes are $\theta_{in} = 22^o$ and $\theta_{out} = 14^o$.

The air-jet experimental facility consists of a centrifuge fan connected to a copper pipe having diameter of 40 mm and length of 1 m. A honeycomb was mounted upstream of the nozzle at the end of the pipe to reduce the turbulence level at the nozzle exit. To measure the fields of mean velocity, a two-dimensional Dantec Laser Doppler Anemometer system was employed. This system is compact and includes two solid lasers: Nd: YAG of 25 mW providing a monochromatic green beam (514.5 nm) and Sapphire of 22 mW providing monochromatic blue beam (488 nm). The measuring volume at the intersection of laser beams was equal to $0.04 \times 0.045 \times 0.378$ mm^3. The probe allowing determination of two velocity components was mounted on a three-dimensional traverse system controlled by a computer. The measurement uncertainties for the mean velocity components and for the RMS velocities were about 0.06% and 0.3%, respectively.

High-speed visualization in the streamwise and transverse planes was performed by a CCD Nanosense MKII camera and a 4 W Nanopower laser providing a 795 nm laser sheet. The acquisition frequency of the visualization system could attain 5 kHz for a window of 512 × 512 pixels. The air jet flow, for both LDA and high-speed visuali-

LEPTAB, Université de La Rochelle, Avenue Michel Crépeau, 17042 La Rochelle, Cedex 01, France; email: inastase@univ-lr.fr. Original article submitted September 15, 2006. Published in Inzhenerno-Fizicheskii Zhurnal, Vol. 81, No. 1, pp. 102–107, February–March, 2008.

TABLE 1. Exit Conditions

Nozzle geometry	$Q_0 \cdot 10^3$, m^3/sec	U_0, m/sec	$Re_0 \cdot 10^{-3}$
Lobed	4.70	3.74	9.5
Circular	4.82	3.84	9.8

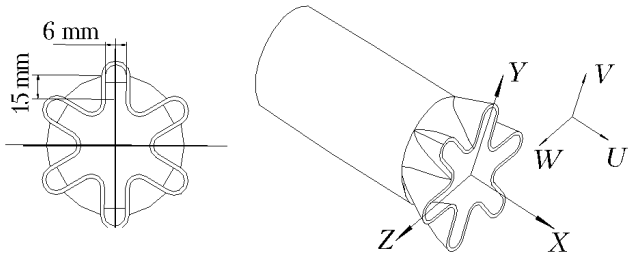

Fig. 1. Lobed nozzle and coordinate system.

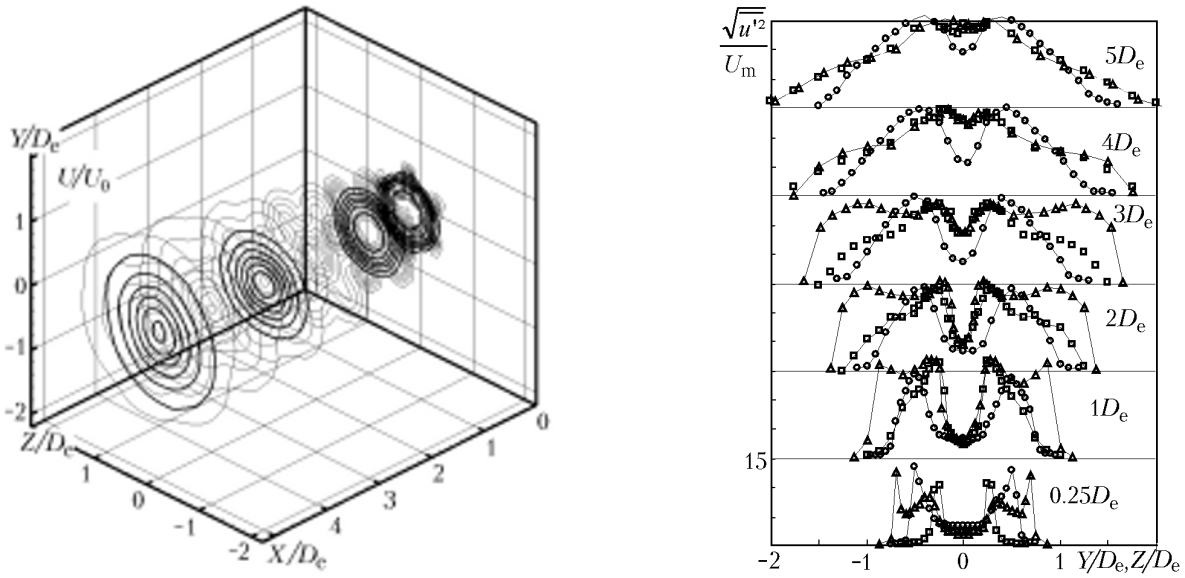

Fig. 2. Superposed contours of the streamwise velocity for the lobed and circular jets.

Fig. 3. Profiles of the intensity of streamwise turbulence: ○ — circular jet; △ —lobed jet, *XY* plane; □ — lobed jet, *XZ* plane. $\sqrt{u'^2}/U_m$, %.

zation, was seeded with small paraffin oil droplets of about 3 μm in diameter supplied by a liquid seeding generator from Dantec.

Table 1 gives the exit conditions for the two nozzles considered. The initial volumetric flow rate calculated from the mean velocity field for the circular and lobed jets revealed a small deviation of the order of 2.5%. The exit Reynolds numbers based on the mean exit velocity U_0 and the equivalent diameter D_e are almost equal for both jets.

Results and Analysis. First, an analysis of the spatial distribution and spreading of the lobed jet compared to the axisymmetric reference jet is made. We present the contours of normalized streamwise velocity for the lobed and circular jets at different axial distances from their exits, which vary from $X = 0.25D_e$ to $X = 5D_e$ (see Fig. 2). The streamwise velocity was normalized by its mean initial value U_0. Two phenomena can be observed in this figure. Unlike the lobed jet, the circular one expands, retaining its nozzle-imposed shape. Indeed, as shown in Fig. 3, the influence of the lobe, which is extremely intense at $X = 0.25D_e$, tends to disappear at $X = 3D_e$. Further downstream, at $X = 5D_e$, contours for the lobed jet become almost circular. However, it can be seen that, compared to the circular jet, its spatial expansion is greater.

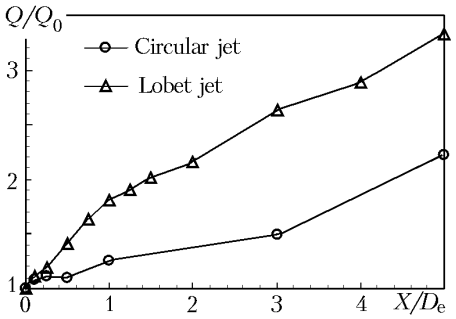

Fig. 4. Streamwise evolution of the volumetric flow rate.

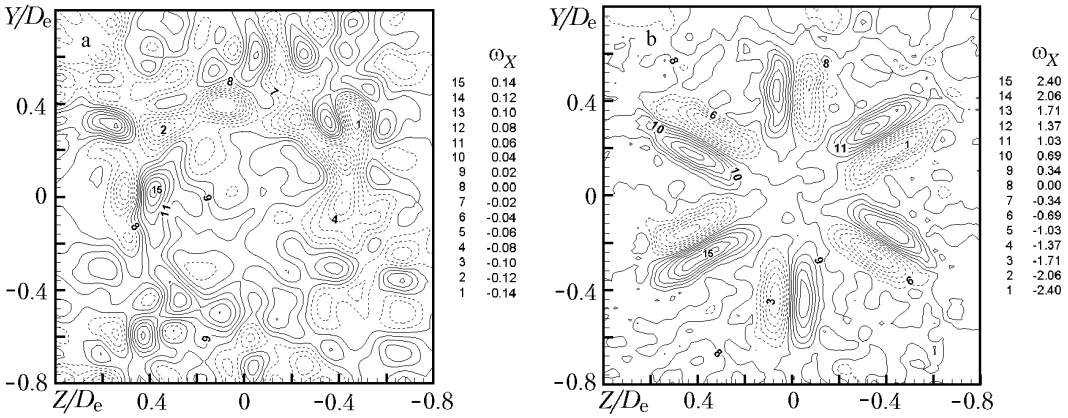

Fig. 5. Fields of the mean streamwise vorticity for circular (a) and lobed (b) jets.

The geometrical change in the lobed jet in the first region can also be seen in Fig. 3, which presents the profiles of streamwise turbulence velocity of the normalized lobed jet compared to the circular one. In the first axial position, a central region of weak turbulence (up to 5%) is present in both jets. Two peaks that could be observed for the circular jet correspond to the shear layer between the jet and the ambient flow. As for the major plane of the lobed jet, the presence of four peaks in the turbulence intensity profile suggests the existence of a doubled shear layer, as we will show later. Very rapidly the central region of weak turbulence, which corresponds to the potential core, becomes very narrow in the lobed jet. From $X = 3D_e$, its corresponding turbulence level begins to rise up and reaches 13% at $X = 4D_e$. We notice that, from the distance mentioned, the axial turbulence rate of the circular jet is hardly higher than its initial level, while in the lobed jet at this distance the given characteristic is much superior to that at the exit.

The evolution of this central zone allows us to place the entire consumption in the potential core of the lobed jet between $3D_e$ and $4D_e$. In the circular jet, the central zone is consumed beyond $X = 5D_e$. The early extinction of the potential core in association with the high spatial expansion and dynamics of the lobed jet enables us to determine its mixing performance and to compare it with that of the circular jet (see Fig. 4). It should be noted that for the circular jet the normalized entrainment rate is quasi-linear and a slope of 0.23 perfectly agrees with the experimental data of [2, 9] that range between 0.21 and 0.25.

As for the lobed jet, the linear approximation of the streamwise evolution of the volumetric rate gives a slope of 0.50, which shows the mixing advantage of the lobed jet over the circular one. This performance is also superior to that for the jet issuing from a circular tabbed nozzle [2], whose flow rate evolution is characterized by a slope of 0.38.

Analysis of the fields of mean streamwise vorticity in the transverse plane at $X = 0.25D_e$ for different values of ω_x (Fig. 5) shows the existence of six pairs of large-scale counter-rotating vortices for the lobed jet, each corresponding to one lobe. These structures have the same spatial scale as the lobes (i.e., they are characterized by the lobe height and by the outer inclination angle of the lobes $\theta_{out} = 14^o$), which amplifies their role in momentum transport. Contrary to the above observations, the streamwise vorticity field for the circular jet does not reveal any organization.

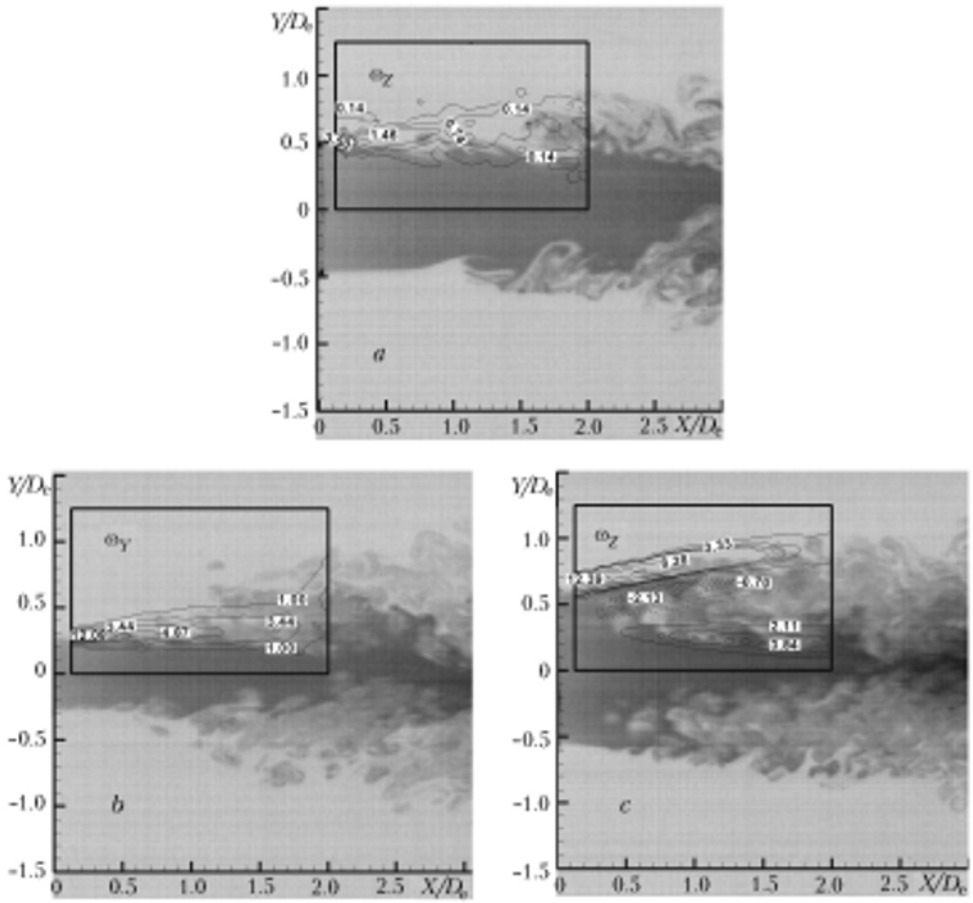

Fig. 6. Contours of the mean azimuthal vorticity superposed on images from high-speed vizualisation: a) circular jet; b) lobed jet, minor plane; c) lobed jet, major plane.

Moreover, the magnitudes of levels of the vorticity are much reduced, so that the ratio between the corresponding maximal values for the lobed and circular jets is equal to 17.

In Fig. 6 we superpose the contours of mean azimuthal vorticity on corresponding images obtained from high-speed visualizations. Here,

$$\omega_Y = \frac{D_e}{U_0}\left(\frac{\partial W}{\partial X} - \frac{\partial U}{\partial Z}\right), \quad \omega_Z = \frac{D_e}{U_0}\left(\frac{\partial V}{\partial X} - \frac{\partial U}{\partial Y}\right).$$

Owing to the symmetry, the contours for only one-half of the flow are presented. The fields of mean azimuthal vorticity in the minor and major streamwise planes, respectively $(XZ)_{Y=0}$ and $(XY)_{Z=0}$, of the lobed jet are compared with the field for the vertical streamwise plane $(XY)_{Z=0}$ of the circular jet up to $X = 2D_e$, which completes the previous analysis.

As expected, the circular jet (Fig. 6a) presents one region, where the values of azimuthal vorticity are positive. This region corresponds to the shear layer, where the vortical structures, due to the Kelvin–Helmholtz instability, are detaching. These induction-generating vortices are shed parallel to the jet axis from the nozzle lip at the vertical distance $Y = 0.5D_e$.

As for the field of mean vorticity for the lobed jet, there are several interesting aspects that could be observed (Fig. 6b and c). First, when facing the minor plane of the lobed jet, we could observe, as in the case of the circular jet, the presence of one positive vorticity region corresponding to the roll-up of the Kelvin-Helmholtz structures detaching at the lobe trough (Fig. 6b). It should also be noted that this phenomenon seems to be more intense than for

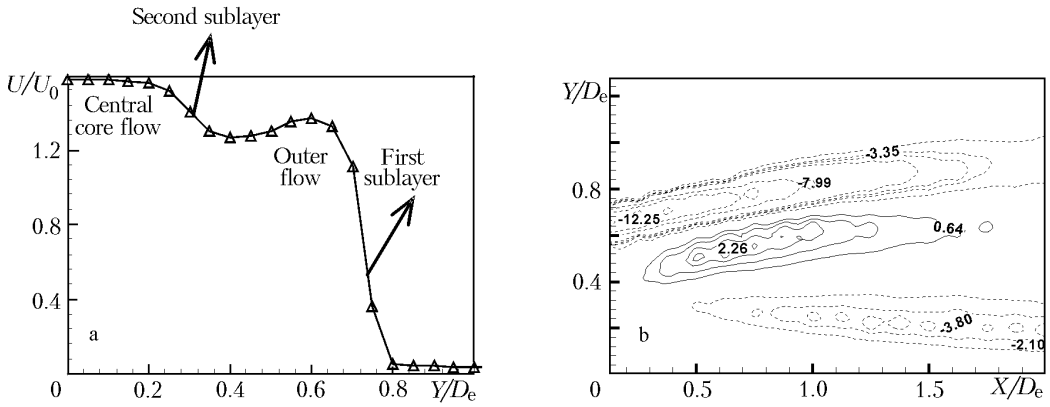

Fig. 7. Profile of the normalized streamwise velocity in the half major plane of the lobed jet at $X = 0.5D_e$ (a) and contours of $\frac{D_e}{U_0}\left(\frac{\partial U}{\partial Y}\right)$ in the half major plane of the lobed jet (b).

the circular jet, since the maximal values of vorticity are more than three times higher. Moreover, on high-speed visualization images one could observe that the vortices detaching in the minor plane of the lobed jet have smaller scale and that they occur earlier.

In the major plane, the mean vorticity field (Fig. 6c) confirms that the shear layer between the flow in the jet core and the ambient flow is divided into two sublayers: the first between the ambient flow and the outer flow of the jet and the second between the latter and the central core flow (Fig. 7a). In the outer flow of the jet, the streamwise velocity U is nonuniform, but it increases slowly (Fig. 7a), which explains the presence of a region where the values of $\frac{\partial U}{\partial Y}$ are positive (Fig. 7b). We see from a comparison of Figs. 6c and 7b that it is easy to observe that $\frac{\partial U}{\partial Y}$ is the preponderant term in the vorticity component ω_Z in the major plane of the lobed jet, and the negative values of ω_Z (Fig. 6c) could be associated with the slight increase of the velocity in the outer flow of the jet.

As for the inner shear layer, its presence is caused by the roll-up of the azimuthal vortical structures detaching in the lobe troughs and shedding towards the interior region of the flow due to the inner penetration angle $\theta_{in} = 22^o$. Furthermore, the normal vortices [10] detaching at the lobe sides are probably contributing to this internal shear. The trajectory inclination of the resulting outer flow of the jet, which is visible in Fig. 6c, agrees with the outer penetration angle of the lobe $\theta_{out} = 14$.

Conclusions. We have presented the results of an experimental investigation of a turbulent isothermal air lobed jet flow. Mixing performance and spreading in the near field of the flow in this jet were analyzed and compared with those for a circular jet of the same initial Reynolds number. It has been shown that the streamwise variation of the volumetric flow rate of the lobed jet reveals a slope which is more than twice larger than that for the reference circular one. This slope is also superior to the slope reported in the literature for a jet issuing from a circular tabbed nozzle. This high entrainment rate is, at the same time, due to the turbulent structures generated by the nozzle of asymmetric shape and to the high convection of these structures induced by the inner and outer penetration angles of the lobes.

NOTATION

D, circular nozzle diameter, mm; D_e, equivalent diameter of a lobed nozzle, mm; H, lobe height, mm; Q, volumetric rate of jet flow, m^3/sec; Re, Reynolds number; U_0, initial mean velocity, m/sec; U_m, centerline velocity, m/sec; U, V, and W, mean streamwise, vertical, and lateral velocity components, m/sec; X, Y, Z, Cartesian coordinates, mm; $\sqrt{u'^2}$, RMS of the streamwise velocity fluctuation, m/sec; λ, lobe width, mm; ω_X, ω_Y, and ω_Z, mean streamwise,

vertical, and lateral normalized vorticity components; θ_{in} and θ_{out}, inward and outward penetration angles of the lobe. Subscripts: 0, initial value; overbar, mean value.

REFERENCES

1. K. B. M. Q. Zaman, Axis switching and spreading of an asymmetric jet: the role of coherent structure dynamics, *J. Fluid Mech*., **316,** 1–27 (1996).
2. K. B. M. Q. Zaman, Spreading characteristics and thrust of jets from asymmetric nozzles, *AIAA Paper,* No. 96–0200 (1996).
3. H. Hu, T. Kobayashi, S. Wu, and G. Shen, Changes to the vortical and turbulent structure of jet flows due to mechanical tabs, *Proc. Inst. Mech. Eng*., **213**, Part C, 321–329 (1999).
4. H. Hu, T. Saga, T. Kobayashi, and N. Taniguchi, Passive control on jet mixing flows by using vortex generators, in: *Proc. 6th Triennial Int. Symp. on Fluid Control, Measurement, and Visualization,* Sherbrooke, Canada (2000).
5. V. M. Belovich and M. Samimy, Mixing processes in a coaxial geometry with a central lobed mixer-nozzle, *AIAA J.,* **35**, No. 5, 838–841 (1997).
6. Y. Yuan, *Jet fluid mixing control through manipulation of inviscid flow structures,* Ph.D. Thesis, Virginia Polytechnic Institute and State University (2000).
7. H. Hu, T. Saga, T. Kobayashi, and N. Taniguchi, A study on a lobed jet mixing flow by using stereoscopic particle image velocimetry technique, *Phys. Fluids,* **13**, No. 11, 3425—3441 (2001).
8. K. B. M. Q. Zaman, F. Y. Wang, and N. J. Georgiadis, Noise, turbulence and thrust of subsonic free jets from lobed nozzles, *AIAA J.,* **41**, No. 3, 397–407 (2003).
9. K. B. M. Q. Zaman, Flow field and near and far sound field of a subsonic jet, *J. Sound Vib*., **106**, 1–16 (1986).
10. D. C. McCormick and J. C. Benett Jr., Vortical and turbulent structure of a lobed mixer free shear layer, *AIAA J.,* **32**, No. 9, 1852–1859 (1994).